

Pore Structure Indicators of Chloride Transport in Metakaolin and Silica Fume Self-Compacting Concrete

Parviz Ghoddousi¹ · Leyla Adelzade Saadabadi¹

Received: 3 October 2016 / Revised: 10 January 2017 / Accepted: 25 January 2017 / Published online: 4 April 2017
© Iran University of Science and Technology 2017

Abstract The aim of this paper is to investigate the microstructure indicators and more effective durability mechanisms of SCCs (Self-Consolidating Concretes) containing supplementary cementitious material. The reference SCC mixture at constant water-to-cementitious material (W/CM) ratio of 0.45 and total cementitious material content of 450 kg/m³ was prepared. The other mixes containing binary (92% PC + 8% SF, 88% PC + 12% SF, and 80%PC + 20%MK) and ternary (72%PC + 8%SF + 20%MK) cementitious blends of metakaolin and silica fume were studied. The effect of using MK and SF in SCCs made with binary and ternary cementitious blends of metakaolin and silica fume and cement on chloride transport and electrical properties was investigated by measuring electrical resistivity parameters such as pore surface conductivity, pore solution conductivity, and tortuosity of pores as chemical and physical indicators of durability. Observations indicated a stronger relationship between the chloride migration coefficient and pore surface conductivity. A new parameter $\tau\sigma_s$ (multiplication of tortuosity and pore surface conductivity), called pore chemi-physical factor, was introduced. Results indicate that the addition of pozzolanic materials such as silica fume and metakaolin leads to a remarkable increase in pore surface conductivity. The correlation coefficient between $\tau\sigma_s$ and the chloride migration coefficient was 0.97. So, if chloride ions are absorbed by pore surfaces,

the chloride migration coefficient will decrease in greater tortuosity.

Keywords Chloride transport · Electrical resistivity · Pore surface conductivity · Supplementary cementitious material

1 Introduction

Due to its effects on durability performance of cementitious materials, pore structure is a key factor in explaining the moisture and ionic transport phenomenon [1, 2]. Moisture and ionic transport into concrete govern the service life of reinforced concrete structures [3–5]. In concrete technology, it is known that the mechanism of failure begins by fluid penetration into micropores of the concrete. Concrete durability is influenced by processes, in which particles such as ions or molecules enter and pass through pores within liquids, while gases fill the voids.

Total porosity of cement-based materials is the most prevalently employed pore structure characteristic of concretes. According to Neithalath and Jain's study [6], moisture intake parameters such as sorptivity are functions of porosity. Previous studies have reported that the use of up to 9% by mass of silica fume as a cement substitution material eventuates in a noticeable alteration of pore structure, including remarkable reduction in pore sizes and connectivity of the cement pastes or concretes [7, 8]. The other combined microstructural parameter is $\phi\beta$ (product of porosity and pore connectivity), which is used to relate the pore structure to the moisture and ionic transport [9]. The use of silica fume leads to an even more remarkable reduction in pore sizes and connectivity than a reduction in the porosity [7, 10]. As illustrated by Cam and Neithalath [9],

✉ Parviz Ghoddousi
Ghoddousi@iust.ac.ir

Leyla Adelzade Saadabadi
Leyla_Adelzade@civileng.iust.ac.ir

¹ School of Civil Engineering, Iran University of Science and Technology, Tehran, Iran

the incorporation of silica fume as a cement replacement material lessens the pore solution conductivity because of decreased concentration of the highly conductive Na⁺ and K⁺ ions, and reduces $\varphi\beta$, because of the pore filling and pozzolanic effect of silica fume particles. However, based on the experimental results, pore connectivity is found to be much more efficient in the alteration of chloride transport than porosity [6]. According to Grathwohl's "Diffusion in Natural Porous Media"[11], tortuosity is a microstructural parameter that is explained as the type of "fudge" factors in macroscopic transport equations to calculate complicated transport paths in porous substances. This complicated parameter is described by the percolating pore space, which controls the transport properties in cement pastes.

In addition to microstructural parameters as mentioned before, Glass and Buenfeld [12] introduced a parameter, according to the types of interaction between different ions and pore walls, which influences the chloride movement into concrete. Two types of interactions exist between chloride ions and pore walls, a chemical chloride binding that is dominated by the aluminate phase, and a physical binding where chloride ions can bind to pore walls without any chemical compositions (the surface forces lead the chlorides to bind to pore walls) [13–15].

In other words, the main chemical and physical phenomena occur in cement-based materials. Examples include the chemical binding by pore solution and the electrostatic interaction between ions contained in the pore solution and the electrical double layer (EDL). The electrocapillary process between pore wall surfaces and pore solution is referred to as the electrical double layer. This phenomenon causes a viscous electric effect that leads to decreased chloride movement [16]. Chatterji and Kawamura [17] were the first to launch a qualitative study on the EDL influence on the ionic transport properties of cement-based materials. Nguyen and Amiri [18] have simulated chloride profiles in concrete by incorporating fly ash and slag to illustrate the influence of electrical double layer on chloride ingress. Different methods have been used to investigate this issue and its relationship between EDL and ionic transport. In the present study, a microstructural parameter σ_s (the electrical conductivity of pore surface) [19] based on the EDL concept from electrical conductivity was considered as an indicator of the electrical double layer. The relationship between σ_s and chloride migration coefficient was analyzed in order to show how the electrical double layer affects the chloride movement.

The durability of SCCs with or without supplementary cementitious material was studied in pervious publication [20–23]. There is the lack of studies on the microstructural and electrical resistivity properties of SCCs containing silica fume and metakaolin. Influences of MK and SF were also studied in self-compacting concretes made with

binary and ternary cementitious blends of metakaolin and silica fume on chloride ion transport properties by measuring electrical resistivity parameters such as pore surface conductivity, pore solution conductivity, shape formation, and pore tortuosity in the present study.

2 Durability Indicators: Chemical and Physical Microstructure Indicators

Electrical mensuration is employed as a non-destructive test to evaluate the durability properties of materials. The micropore structure properties, which can be calculated in this test by electrical measurement methods, include porosity, pore connectivity, water permeability, and ion diffusivity [24, 25]. Also, electrical measurement procedures have been suggested to scan water and ionic transportation into concrete [26–30]. Electrical specification is thus considered a durability indicator. Several models have described the electrical conductivity of the composite system [19, 31]. The most important of these models, which incorporates a composite system in distinct phases, is the effective electrical conductivity; see Eq. 1 [19]:

$$\sigma_t = \sum_{i=1}^n (\sigma_i \varphi_i \beta_i), \quad (1)$$

where σ_i , φ_i , and β_i , are the electrical conductivity, volume fraction, and the connectivity factor of each component(i), respectively.

Since pore solution in concrete is conductive, Eq. 1 can be simplified and changed into Eq. 2 [19, 32]:

$$\sigma_t = \sigma_0 \varphi \beta, \quad (2)$$

where σ_0 is the pore solution conductivity and φ is the total porosity (some studies suggested capillary pores, while the others, total porosity).

According to equations 1 and 2, it is essential to identify the formation factor constituting total porosity and pore interconnectivity as an effective parameter in the electrical resistivity of concrete. The Nernst–Einstein's Equation was used:

$$\frac{\sigma_{\text{pore}}}{\sigma_t} = \frac{D_0}{D_{\text{eff}}} = F, \quad (3)$$

where σ_t , σ_{pore} , D_{eff} , and D_0 are the total electrical conductivity of concrete, electrical conductivity of pore solution, effective chloride migration coefficient, and chloride self-diffusion coefficient in water, respectively, and F is the inverse of the formation factor ($\varphi\beta$) [6, 32]. See Eq. 4 [6].

In this study, the formation factors of all mixes were calculated with relative chloride migration coefficients (D_{eff}/D_0) and relative electrical conductivity ($\sigma_{\text{eff}}/\sigma_{\text{pore}}$).

When determining the physical and geometrical specifications of pores, pore conductivity in concrete, and the manner in which pore solution can move in and fill voids, one cannot depend solely on the total porosity volume and its geometry, but also on the tortuosity of connected pores [6]. Accordingly, the value of connected pore tortuosity can be defined as the function of porosity and formation factor [33]:

$$\tau^2 = \frac{\sigma_{\text{pore}}}{\sigma_t} \phi, \tag{4}$$

where τ is the tortuosity, based on equations 3, 4:

$$\tau = \beta^{-1/2}. \tag{5}$$

Rajabipour and Weiss [19] suggested that the electrical conductivity of concrete specimens does not depend solely on pore electrical conductivity, but also on a new parameter, introduced as the electrical conductivity of pore surfaces; see Eq. 6 [19]:

$$\sigma_t = \beta \left(\sigma_0 \phi + \sigma_s \phi \left(\frac{2}{\Lambda} \right) \right), \tag{6}$$

where σ_s is the electrical conductivity of pore surfaces and $(2/\Lambda)$ is a microstructural parameter of the surface-to-volume ratio of the pore.

Several chemical and physical phenomena occurring in cement-based materials are crucial to the understanding of water and chloride transport, including chemical binding, pore solution activity, and electrostatic interaction between the ions involved in pore solution and EDL. The electrocapillary process between pore wall surfaces and pore solution is referred to as the electrical double layer. This process causes a viscous electric effect that leads to a decrease in chloride movement [16]. For purposes of this study, a microstructural parameter σ_s (the electrical conductivity of pore surface) [19] based on EDL concept

from electrical conductivity was considered as an indicator of the electrical double layer to show how the electrical double layer affects chloride movement. The relationship between σ_s and the chloride migration coefficient was discussed.

3 Experimental Program

3.1 Materials

In this study, a locally available type II Portland cement and limestone powder were used to develop self-compacting concrete mixes. Table 1 shows the chemical characteristics of the cementitious materials used in the mixes. Self-compacting concrete mixtures are generally made from natural river sand with a specific density of 2.44 and water absorption of 3.1% as fine aggregate and 19 mm maximum size stone of 2.54 specific density, and coarse aggregates of 1.8% water absorption. Figure 1a, b shows the used aggregate grading for SCC mixes and limestone powder.

A polycarboxylate superplasticizer with a density of 1.01 g/cm³, referred to as the p100 and produced by the Shimisakhteman Co., was used to achieve the SCC workability requirements according to EFNARC [34].

3.2 Mixture Proportion

Five self-compacting concrete mixtures were designed to be used in this work. The water-to-cementitious material ratio of mixtures was kept at a constant of 0.45 and a total cementitious material content of 450 kg/m³ was considered. The reference mixture contains 450 kg/m³ of cement without any pozzolan. The other mixes contained binary (92% PC + 8% SF and 88%PC + 12%SF, 80%PC + 20%MK) and ternary (72%PC + 8%SF + 20%MK) cementitious blends,

Table 1 Chemical characteristics of cementitious materials

Chemical composition	Cement (%)	Silica fume (%)	Metakaolin (%)	Limestone powder (%)
SiO ₂	20.74	94.00	52.80	2.80
Al ₂ O ₃	4.90	1.00	36.30	0.35
Fe ₂ O ₃	3.50	0.10	4.21	0.50
MgO	1.20	0.60	0.81	1.80
CaO	62.95	1.00	0.10	51.22
SO ₃	3.00	1.20	–	1.24
K ₂ O	–	–	–	–
Ignition loss	1.56	–	3.53	42.06
Free lime	0.74	–	–	2.8
Physical property				
Specific density (kg/m ³)	3150	2200	2600	2660

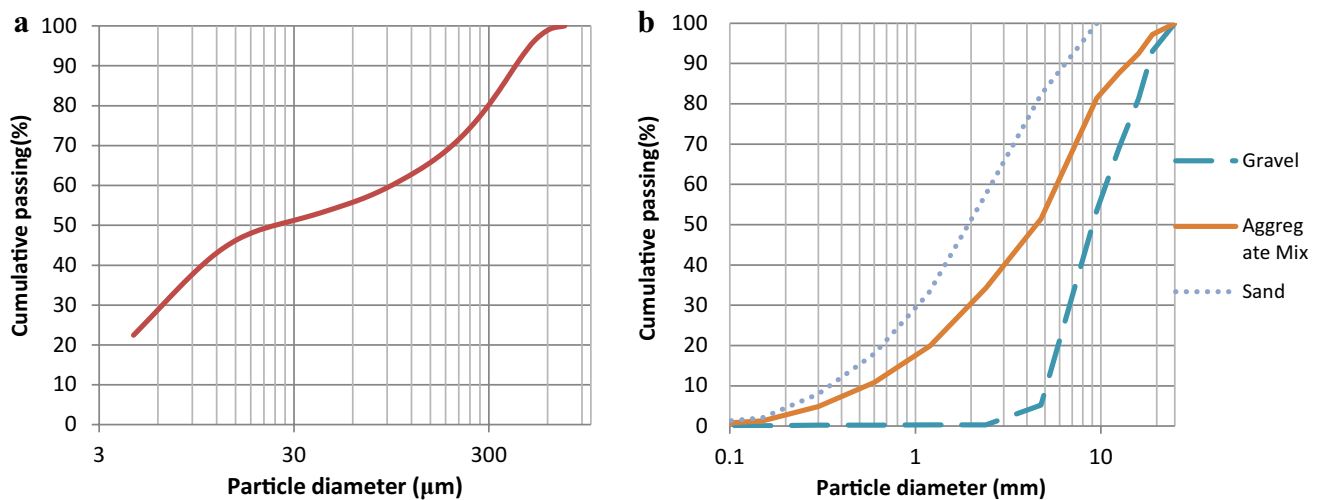


Fig. 1 **a** Particle size distribution of filler (limestone powder) and **b** sand, gravel, and aggregate mix grading

where the proportions of Portland cement in mass were replaced with SF and MK. Details of the mixtures and compressive strength of SCCs are shown in Table 2. After casting the required specimens according to test procedures, all samples were left to set for 24 h, before demolding; they were then cured in a water tank for 28 days at 20 °C.

4 Test Procedure

4.1 Workability Properties

After mixing occurs, self-compacting concrete procedures such as slump flow, V-funnel, J-ring, and L-Box are conducted to meet the European Federation of National Associations Representing for Concrete (ENFARC) [34] SCC workability requirements.

4.2 Mercury Intrusion Porosimetry (MIP)

Total porosity and pore size distribution curves were measured by mercury intrusion porosimetry (Thermo Finnigan, Pascal 440) with a maximum pressure of 207 Psi. The contact angle was 140° and the measurable pore size ranged from about 5 nm to 1000 μm. The samples, which were about 5 mm in size, were separated from the crushed specimens for pore structure testing. In order to avoid dehydration, the samples were dried at about 105 °C for 24 h before the MIP test.

4.3 Electrical Resistivity Test

The electrical resistivity test was conducted on three cube specimens (100×100×100 mm) after 28 days of curing.

The test makes it possible to measure the electrical resistivity parameters such as pore surface conductivity, pore solution conductivity, shape formation, and pore tortuosity. Two plates of brass were used as two electrodes on the saturated surfaces of dry samples to measure the electrical resistivity by a specific ohm meter. Normally, a thin layer of loose cement paste is used in binding to connect concrete and brass plates.

4.4 Pore Solution Analysis

To measure the electrical conductivity of pore solution, powder samples of each specimen were drilled and dissolved in a certain amount of water. Pore solution conductivity was obtained by recording the solution's electrical resistivity, and calibration with the saturation degree of samples which M_s is the powder mass, M_w is the amount of water in which the powder was dissolved, Φ is the open porosity, σ_{pore} is the solution's electrical conductivity, M_{SSD} is the SSD mass of cubic samples of each concrete, and $\sigma_{\text{pore(real)}}$ is the electrical conductivity of pore solution. It was supposed that free ions within the pore solution were released in water after 24 h.

4.5 Pore Surface Conductivity Measurement

To determine the pore surface conductivity of concrete samples, the relationship between the overall conductivity (from electrical resistivity test) and the pore solution conductivity (from pore solution analysis) was observed for each concrete sample at a saturated surface-dried state (equations 2–6).

4.6 Rapid Chloride Migration Test

The rapid chloride migration test was carried out according to NT BUILD 492 (See Fig. 2). The chloride migration coefficient was determined according to the Guideline NT BUILD 492 (Eq. 7).

$$D_{Cl} = \frac{0.0239(273 + T)L}{(U - 2)t} \left(x_d - 0.0238 \sqrt{\frac{(273 + T)Lx_d}{U - 2}} \right), \tag{7}$$

where D_{Cl} is the chloride migration coefficient, m^2/s ; U is the applied voltage, V ; T represents the average initial and final temperatures in the catholyte solution, $^{\circ}C$; L is the thickness of the specimen, mm ; x_d is the average of penetration depths, mm ; and t is the test duration, hour.

5 Results and Discussion

5.1 Workability

Fresh properties of self-compacting concrete mixtures are presented in Table 3. These results indicated that



Fig. 2 NT BUILD 492 set-up

Table 2 Mixture proportions and compressive strength of self-compacting concrete

Mix	W/Cm	Cement	SF	MK	LP	Aggregate	SP	Compressive strength (28 days)
		kg/m ³					(l)	(MPa)
S-Ref	0.45	450	0	0	150	1497	1.43	35.3
S-SF	0.45	414	36	0	150	1483	2.28	50.4
S-SF-2	0.45	396	54	0	150	1476	2.57	37.1
S-MK	0.45	360	0	90	150	1477	3.42	81.8
S-SF/MK	0.45	324	36	90	150	1463	3.42	82.3

all mixtures have acceptable workability according to EFNARC [34].

5.2 Porosity

Results of the pore structure measured by MIP are shown in Table 4. The pore size distribution curves of SCCs are presented in Figs. 3 and 4. The S-Ref showed the highest porosity. The pore distribution curve of other SCCs is slightly different. The pore size distribution curve of S-Ref (plain SCC) showed the significant volume of the pores to be 100 nm. This curve reached a plateau of less than 10 nm; device limitations, no more than 3 nm in pore diameter, illustrated the majority of pores to range from 10 to 100 nm in size. Pores measured to be larger than 10 nm are called capillary pores [35]. The S-MK curves showed a steady decrease down to 3 nm (the equipment’s measurement limit). This indicated that the volume percentage of pores might not be intruded by mercury, even at the maximum pressure of 207 psi, and most fraction pores are finer than 3 nm. The considerable difference between the average pore diameter of reference SCC and that of others showed the range of pore size in SCCs containing SCM to be much wider and finer, while the total porosities of SCCs containing SCMs were higher than that of S-Ref. Specific surface of S-MK and S-SF/MK pores showed the highest amount. It can be argued that MK and SF/MK combination as a replacement of Portland cement causes finer pores. It can be noticed that SCCs incorporating binary and ternary

Table 3 Fresh properties of self-compacting concrete mixtures

Mix	Slump flow (mm)	T50 (s)	J-ring (mm)	V-funnel	L-box flow (mm)
S-Ref	640	1.18	5	3.57	0.9
S-SF	730	2.14	5	11.11	0.9
S-SF2	640	0.99	7	3.35	0.85
S-MK	730	2.59	3	8.84	1
S-SF/MK	710	1.59	5	5.46	0.9

Table 4 Results of pore structure measured by MIP

Mix	Total cumulative volume (mm ³ /g)	Total specific surface area (m ² /g)	Average pore diameter (nm)	Total porosity (%)
S-Ref	63.6464	11.997	104.15	14.41
S-SF	71.9737	23.662	6.13	16.8
S-SF2	105.230	26.33	5.48	16.79
S-MK	73.6957	23.698	5.27	16.91
S-SF/MK	88.3077	31.151	5.93	20.07

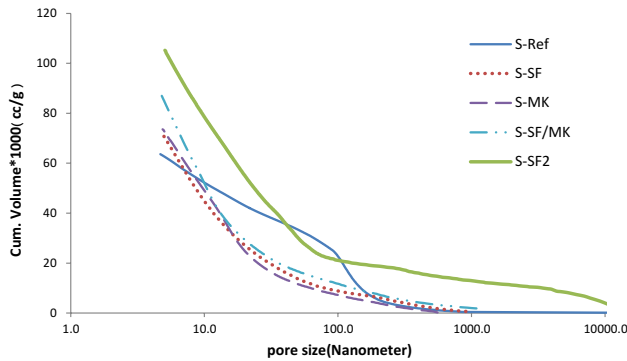


Fig. 3 Cumulative volume of pores of SCCs

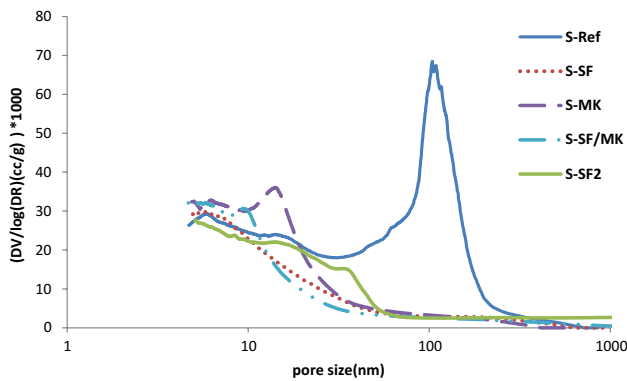


Fig. 4 Pore size distribution curves of SCCs

Table 5 Chemical and physical pore indicators

Mix	$\varphi\beta$ (D/D_0)	$\varphi\beta$ (σ/σ_0)	β	τ	σ_s (μ S)	σ_0 (S/m)
S-Ref	0.0060	0.035	0.042	4.90	1.85	2.10
S-SF	0.0059	0.015	0.035	5.35	792.69	1.54
S-SF2	0.0152	0.047	0.064	3.96	159.34	0.61
S-MK	0.0054	0.024	0.032	5.59	424.76	0.74
S-SF/MK	0.0031	0.039	0.016	8.00	217.25	0.24

blends of MK and SF showed only a small volume of pores to be larger than 1000 nm.

5.3 Durability Indicators: Micropore Structural Parameters

Pore shape and tortuosity factor, pore conductivity, and pore surface conductivity were calculated and are listed in Table 5. The different values of the relative chloride migration coefficient (D_{eff}/D_0) and the relative electrical conductivity ($\sigma_{eff}/\sigma_{pore}$) presented in Table 5 prove that the suggestion of Rajabipour and Weiss [19] can be applicable to concrete containing SCMs. Rajabipour and Weiss [19] suggested that the electrical conductivity of concrete specimens does not depend solely on pore electrical conductivity, but also on a new parameter, introduced as electrical conductivity of pore surfaces. The incorporation of 8% silica fume as a replacement of cement results in a reduction of $\varphi\beta$ values. However the alteration is not considerable. The addition of 12% silica fume instead of cement caused an increase of up to about 250% of $\varphi\beta$ value. No significant alteration in the $\varphi\beta$ values of SCC containing MK as a cement replacement was observed. The $\varphi\beta$ value of SCC, containing ternary cementitious blends of metakaolin and silica fume, has had a noticeable reduction compared to that of the SCC reference. The value of pore shape factor in SCC-SF/MK constitutes only a more half of SCC-Ref. The pore shape factor of two SCCs containing binary cementitious blends of metakaolin and silica fume proved to be approximately the same. This does not mean that the porosity and pore conductivity values of the above-mentioned SCCs are similar.

As shown in Table 4, total porosity of the reference SCC was less than those of SCC-SF and SCC-MK. Therefore, the value of pore connectivity in SCCs modified with binary cementitious blends of metakaolin and silica fume are higher compared to SCCs without any SCMs. Compared to SCC-Ref, the incorporation of silica fume in SCC mixes results in a remarkable pore connectivity reduction; this is mainly due to the pore filling and pozzolanic effects of silica fume. Previous studies have

shown that the addition of silica fume (up to 9% mass) as a cement replacement material results in significant pore size and connectivity reduction of cement pastes or concretes [7, 8].

5.4 Pore Connectivity and Pore Tortuosity

The pore connectivity and pore tortuosity of SCC mixes, which are physical geometrical indicators of pore structure, are presented in Fig. 5. As mentioned before, it does not mean that the porosity and pore conductivity values are equal; the durability specifications of SCC mixes are therefore similar when their pore shape values are the same. The pore connectivity value of SCC-Ref is 0.042, while SCC mixes modified with binary cementitious blends of silica fume and metakaolin are 25% less in comparison with reference SCC (0.034, 0.032). But when the SCC mix was prepared with 12% silica fume as a cement replacement, pore connectivity increased up to 0.063. Results show that the SCC containing both metakaolin and silica fume has the lowest pore connectivity. The incorporation of ternary cementitious blends of metakaolin and silica fume in SCC mixes resulted in a noticeable reduction in pore connectivity, which was not observed in SCC mixes that lacked modification materials. This is mainly due to the pore filling and pozzolanic effects of silica fume and metakaolin. However, when cement is replaced with silica fume greater in mass by 8% of the cement’s weight, the silica fume continues to react, while low pH values and the absence of portlandite work to destabilize the monocarbonate [36]. Calculations by lothenbach et al. [37] indicate that, upon further replacement of PC by silica fume (or upon further reaction of the silica fume), ettringite will become unstable.

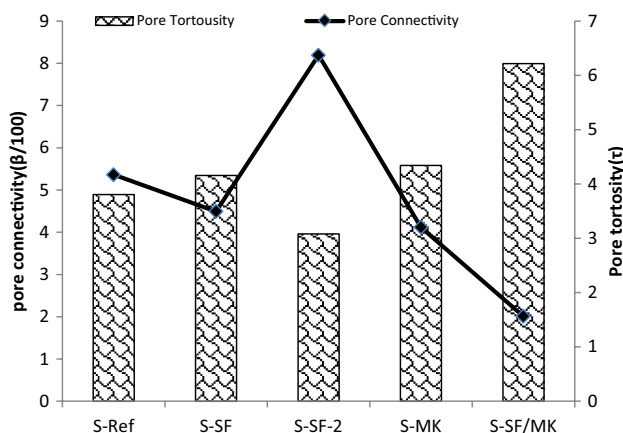


Fig. 5 Pore connectivity and pore tortuosity of SCC mixes

According to Grathwohl’s publication [11] on “Diffusion in Natural Porous Media,” tortuosity, the other microstructural parameter, is described as a type of “fudge” factor in macroscopic transport equations to account for the complicated transport paths in porous substances. This complicated parameter is described by the percolating pore space that controls the transport properties in cement pastes. When compared to SCC-Ref, pore tortuosity of SCC mixes, presented in Fig. 5, indicates that the use of silica fume and metakaolin as a cement substitution leads to a significant increase in pore tortuosity.

5.5 Pore Solution Analysis

To investigate the chemical pore structural parameters of SCC mixes, pore solution conductivity and pore surface conductivity were calculated and analyzed. Figure 6 shows pore solution conductivity and pore surface conductivity of SCCs. The pore solution conductivity value of SCC-Ref is 2.1 S/m, which is the highest. Because pore surface conductivity of SCC-Ref is much lower than its pore solution conductivity, it can be ignored. Addition of pozzolanic materials such silica fume and metakaolin leads to a remarkable increase in pore surface conductivity. Incorporation of 8% silica fume as a cement substitution results in the reduction of pore solution conductivity. This indicates that free ion concentrations of K+ and N+ in pore solution are low and therefore reach the pore surface, causing pore surface conductivity to increase. Cam and Neithalath [9] have shown that the incorporation of silica fume as a cement replacement material lessens the pore solution conductivity because of decreased concentration in highly conductive Na+ and K+ ions, and reduces $\phi\beta$ because of pore filling and pozzolanic effects of silica fume particles.

Compared to SCC without any pozzolanic replacements, the use of 8% silica fume leads to reduced pore

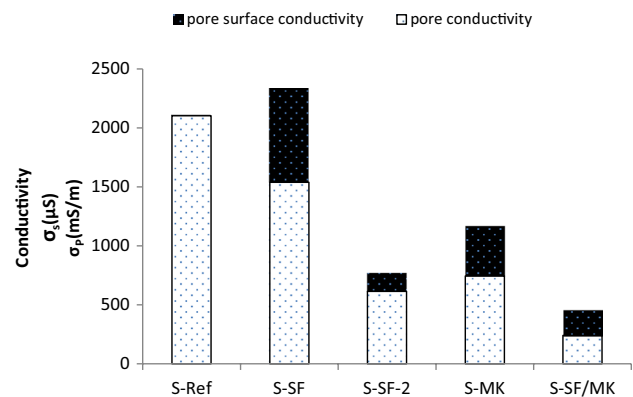


Fig. 6 Pore surface σ_s (μ S) and pore solution σ_p (mS/m) conductivity of SCC mixes

solution conductivity up to 30% and increases the value of pore surface conductivity to 792 μS . According to the present study, the microstructural parameter σ_s (the electrical conductivity of pore surface) based on EDL concept from electrical conductivity was considered as an indicator of the electrical double layer. In other words, using silica fume in SCC mixes results in an EDL increase. It is known that the pozzolanic actions alter the microstructure of C-S-H, and it can be followed by changes in the electrical binding capacity of pore surface conductivity, as well as the physical pore properties [38]. The partial replacement of cement with silica fume affects the C-S-H in three ways [39]: (1) increased C-S-H volume, (2) C_3A dilution, which leads to reduced chloride binding capacity, and (3) pH value reduction, which leads to increased chloride binding capacity. An increase in the pH of the pore solution leads to an increase in the solubility of Friedel's salt; so it causes the release of chloride to the pore solution and the amount of chemically bound chloride can be reduced [40]. Results show that the addition of SF as a partial replacement of Portland cement leads to increased pore surface electrical resistivity. Increased electrophysical absorption of chloride ions on C-S-H surfaces may occur. The chemical pore structure values (σ_s , σ_o) of SCC containing MK are lower than those of SCC mixes modified with silica fume. MK contains a higher amount of Al element which is supposed to have higher chemical chloride binding capacity (Friedel's salt formation), whereas pore surface conductivity is related to electro-physical absorption of chloride ions on C-S-H.

5.6 Relationship Between Durability Indicators

To better understand the effects of micropore structural parameters on macro indicators of chloride diffusion, the relationships between the durability indicators and physical and chemical microstructure indicators of tortuosity and pore surface electrical conductivity are shown in Figs. 7 and 8. The durability indicators include the transport of chloride and electrical resistivity.

It was observed that the relationship between pore tortuosity and chloride migration coefficient was weak (see Fig. 7b). Figure 7a does, however, show a good linear relationship between electrical resistivity and tortuosity, with 0.85 correlation coefficient. It is noteworthy that the electrical resistivity has been significantly governed by tortuosity. Because higher tortuosity leads to a longer path, and decreased electrical conductivity, a long path may cause delay in the movement of several ions.

The results shown in Fig. 8a, b indicate a good relationship between the chloride migration coefficient and the electrical conductivity of pore surfaces, which is the chemical microstructure indicator of durability, but not a good relationship with tortuosity. This observation shows that the migration phenomenon is influenced by chemical microstructural parameters.

From the results, it can be seen that the addition of SF as a partial replacement of Portland cement leads to an increase in the electrical resistivity of pore surfaces. It may result in an increase of electrophysical absorption of chloride ions on C-S-H surfaces. The electrical conductivity of pore surfaces can be an indicator of electrical double layer, as in the presence of pozzolans, which causes the higher electrical charge. Ions have a tendency to absorb to the pore

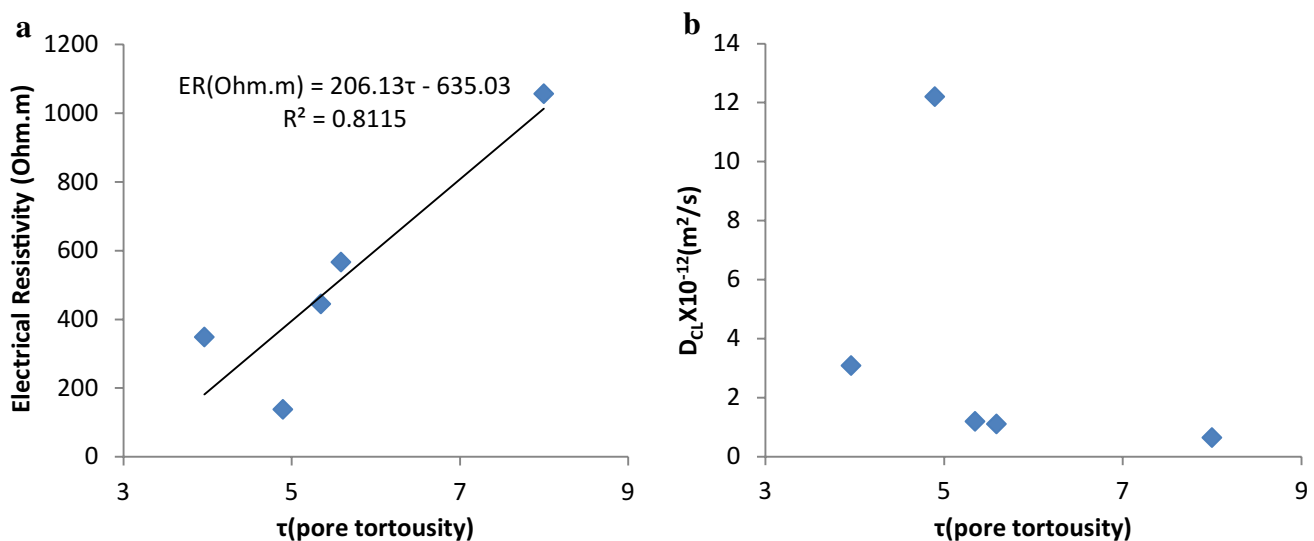


Fig. 7 Relationship of pore tortuosity with (a) electrical resistivity and (b) chloride migration coefficient of SCC mixes

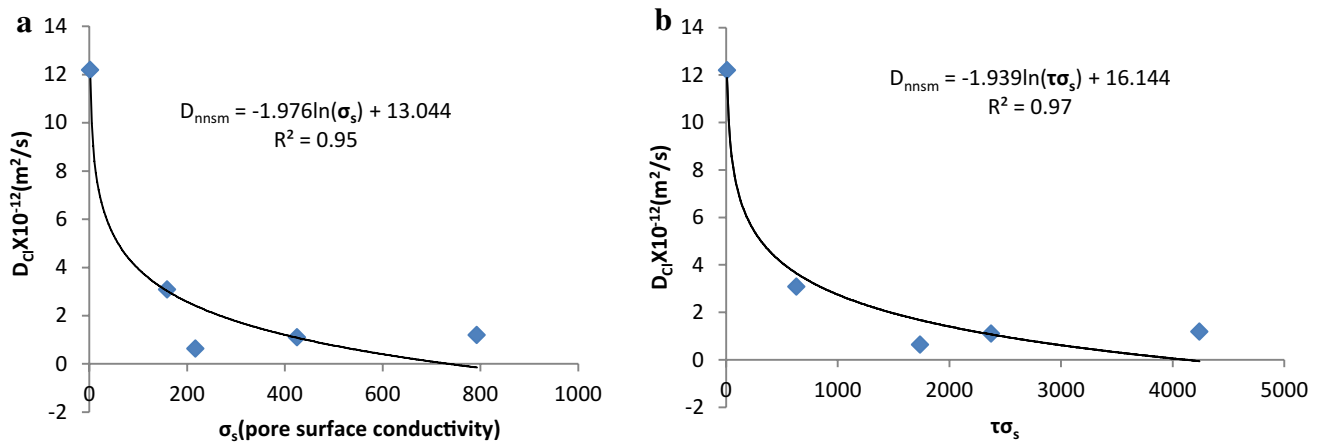


Fig. 8 Relationship of chloride migration coefficient with (a) pore surface conductivity and (b) pore chemi-physical factor of SCCs

surfaces, which can lead to reduced ion transport. The correlation coefficient between $\tau\sigma_s$ and the chloride migration coefficient was 0.97. For purposes of this study, this parameter was referred to as the pore chemi-physical factor. This strong relationship can point out that if chloride ions absorb and bind to the pore surfaces, the chloride migration coefficient will decrease in greater tortuosity.

6 Conclusion

The influences of MK and SF were studied in relation to self-compacting concretes made with binary and ternary cementitious blends of metakaolin and silica fume by measuring new parameters of pore surface conductivity and pore chemi-physical factor. Additionally, chloride ion transport properties, including macro indicators and microstructure indicators of durability, were also studied. The following conclusions can be drawn:

- When compared to SCC-Ref, the pore tortuosity of SCC mixes indicates that the use of silica fume and metakaolin as a substitution of cement leads to significant increases in pore tortuosity.
- Addition of pozzolanic materials such as silica fume and metakaolin leads to a remarkable increase in pore surface conductivity.
- The migration phenomenon is influenced by chemical microstructure parameters, which proved a good relationship between the chloride migration coefficient and pore surface conductivity, but not with tortuosity.
- The correlation coefficient between $\tau\sigma_s$ and the chloride migration coefficient was 0.98. This strong relationship can point out that if chloride ions absorb and bind to the pore surfaces, the chloride migration coefficient will decrease in greater tortuosity.

References

1. Sugiyama T, Ritthichauy W, Tsuji Y (2008) Experimental investigation and numerical modeling of chloride penetration and calcium dissolution in saturated concrete. *Cem Concr Res* 38(1):49–67
2. Sugiyama T, Ritthichauy W, Tsuji Y (2003) Simultaneous transport of chloride and calcium ions in hydrated cement systems. *J Adv Concr Technol* 1(2):127–138
3. Maltais Y, Samson E, and Marchand J, (2004) Predicting the durability of Portland cement systems in aggressive environments—Laboratory validation. *Cem Concr Res*, 34(9):1579–1589.
4. Stanish K, Hooton RD, Thomas MDA (2004) A novel method for describing chloride ion transport due to an electrical gradient in concrete: part 1. theoretical description. *Cem Concr Res* 34(1):43–49
5. Glass GK, Buenfeld NR (2000) The influence of chloride binding on the chloride induced corrosion risk in reinforced concrete. *Corros Sci* 42(2):329–344
6. Neithalath N, Jain J (2010) Relating rapid chloride transport parameters of concretes to microstructural features extracted from electrical impedance. *Cem Concr Res* 40(7):1041–1051
7. Tsivilis S, Tsantilas J, Kakali G, Chaniotakis E, and Sakellariou A, (2003) The permeability of Portland limestone cement concrete. *Cem Concr Res*, 33(9):1465–1471.
8. Igarashi S, Watanabe A, Kawamura M (2005) Evaluation of capillary pore size characteristics in high-strength concrete at early ages. *Cem Concr Res* 35(3):513–519
9. Cam HT, Neithalath N (2010) Moisture and ionic transport in concretes containing coarse limestone powder. *Cem Concr Compos* 32(7):486–496
10. Neithalath N, Persun J, Hossain A (2009) Hydration in high-performance cementitious systems containing vitreous calcium aluminosilicate or silica fume. *Cem Concr Res* 39(6):473–481
11. Grathwohl P Diffusion in natural porous media: contaminant transport, sorption/desorption and dissolution kinetics. Springer US, 2012
12. Glass GK, Buenfeld NR (2000) Chloride-induced corrosion of steel in concrete. *Prog Struct Eng Mater* 2(4):448–458
13. Luping T, Nilsson L-O (Mar. 1993) Chloride binding capacity and binding isotherms of OPC pastes and mortars. *Cem Concr Res* 23(2):247–253

14. Zibara H, Hooton RD, Thomas MDA, Stanish K (2008) Influence of the C/S and C/A ratios of hydration products on the chloride ion binding capacity of lime-SF and lime-MK mixtures. *Cem Concr Res* 38(3):422–426
15. Yuan Q, Shi C, De Schutter G, Audenaert K, Deng D (2009) Chloride binding of cement-based materials subjected to external chloride environment—a review. *Constr Build Mater* 23(1):1–13
16. Friedmann H, Amiri O, Ait-Mokhtar A, Dumargue P (2004) A direct method for determining chloride diffusion coefficient by using migration test. *Cem Concr Res* 34(11):1967–1973
17. Chatterji S, Kawamura M (1992) A critical reappraisal of ion diffusion through cement based materials. Part 1: sample preparation, measurement technique and interpretation of results. *Cem Concr Res* 22(4):525–530
18. Nguyen PT, Amiri O (2014) Study of electrical double layer effect on chloride transport in unsaturated concrete. *Constr Build Mater* 50:492–498
19. Rajabipour F, Weiss J (Dec. 2007) Electrical conductivity of drying cement paste. *Mater Struct* 40(10):1143–1160
20. Kapoor K, Singh SP, and Singh B, (2016) Water permeation properties of self compacting concrete made with coarse and fine recycled concrete aggregates, *Int J Civ Eng*, 1–10, doi:[10.1007/s40999-016-0062-x](https://doi.org/10.1007/s40999-016-0062-x)
21. Meesaraganda LV, Saha P, and Laskar AI, (2016) Behaviour of self-compacting reinforced concrete beams strengthened with hybrid fiber under static and cyclic loading, *Int J Civ Eng*, 1–10, doi:[10.1007/s40999-016-0114-2](https://doi.org/10.1007/s40999-016-0114-2)
22. Ziari H, Hayati P, and Sobhani J, (2016) Air-entrained air field self-consolidating concrete pavements: strength and durability, *Int J Civ Eng*, 1–13, doi:[10.1007/s40999-016-0104-4](https://doi.org/10.1007/s40999-016-0104-4).
23. Sarıdemir M, Severcan MH, Çiflikli M, and Çelikten S, (2016) Microstructural analyses of high strength concretes containing metakaolin at high temperatures. *Int J Civ Eng*, 1–13, doi:[10.1007/s40999-016-0081-7](https://doi.org/10.1007/s40999-016-0081-7).
24. Swamy RN, *Cement Replacement Materials*. Surrey University Press, 1986
25. Karahan O, Hossain KMA, Ozbay E, Lachemi M, Sancak E (Jun. 2012) “Effect of metakaolin content on the properties self-consolidating lightweight concrete”. *Constr Build Mater* 31:320–325
26. Lachemi M, Bae S, Hossain KMA, Sahmaran M (Oct. 2009) Steel–concrete bond strength of lightweight self-consolidating concrete. *Mater Struct* 42(7):1015–1023
27. Güneyisi E, Gesoğlu M, Karaoğlu S, and Mermerdaş K, (2012) Strength, permeability and shrinkage cracking of silica fume and metakaolin concretes. *Constr. Build. Mater.*, 34:120–130
28. Nanthagopalan P, Santhanam M (Mar. 2011) Fresh and hardened properties of self-compacting concrete produced with manufactured sand. *Cem Concr Compos* 33(3):353–358
29. Fernandez R, Martirena F, Scrivener KL (Jan. 2011) The origin of the pozzolanic activity of calcined clay minerals: A comparison between kaolinite, illite and montmorillonite. *Cem Concr Res* 41(1):113–122
30. Coleman NJ, Mcwhinnie WR (2000) The solid state chemistry of metakaolin-blended ordinary Portland cement. *J Mater Sci* 35(11):2701–2710
31. Torquato S *Random heterogeneous materials: microstructure and macroscopic properties*. Springer Science & Business Media, 2013
32. Garboczi EJ (Jul. 1990) Permeability, diffusivity, and microstructural parameters: a critical review. *Cem Concr Res* 20(4):591–601
33. Herrick DC, Kennedy WD (Jun. 1994) Electrical efficiency—A pore geometric theory for interpreting the electrical properties of reservoir rocks. *Geophysics* 59(6):918–927
34. European Federation for Specialist Construction Chemicals and Concrete Systems, “EFNARC, Guidelines for self-compacting concrete.” p. 32, 2002.
35. Yajun J, Cahyadi JH (Oct. 2003) Effects of densified silica fume on microstructure and compressive strength of blended cement pastes. *Cem Concr Res* 33(10):1543–1548
36. Bach TTH, (2010) Evolution physico-chimique des liants bas pH hydrates. Influence de la température et mécanisme de rétention des alcalins, Université de Bourgogne, Dijon, France
37. Lothenbach B, Scrivener K, Hooton RD (Dec. 2011) Supplementary cementitious materials. *Cem Concr Res* 41(12):1244–1256
38. Thomas MDA, Hooton RD, Scott A, Zibara H (Jan. 2012) The effect of supplementary cementitious materials on chloride binding in hardened cement paste. *Cem Concr Res* 42(1):1–7
39. Dousti A, Shekarchi M, Alizadeh R, Taheri-Motlagh A (Nov. 2011) Binding of externally supplied chlorides in micro silica concrete under field exposure conditions. *Cem Concr Compos* 33(10):1071–1079
40. Roberts MH (1962) Effect of calcium chloride on the durability of pre-tensioned wire in prestressed concrete. *Mag Concr Res* 14(42):143–154